ANOMALOUS FATIGUE CRACK GROWTH BEHAVIOUR IN AA 2024 AND AA 5083.

J. ZUIDEMA[(1)], K. VAN KRANENBURG[(1)], T. RIEMSLAG[(1)], F. VEER[(2)] AND S. BOLJANOVIC[(3)]

[(1)]*Laboratory of Materials Science, Delft University of Technology*

[(2)]*Faculty of Architecture, Delft University of Technology*

[(3)]*Faculty of Mechanical (Aircraft) Engineering, University of Belgrade*

ABSTRACT

Fatigue crack growth properties of two aluminum alloys, AA 2024 T351 and AA 5083 H321, are studied. Both materials have been fatigued in various environments and different frequencies using constant-amplitude fatigue crack growth tests. Fatigue crack growth starts in the flat tensile mode, but after some crack advance shear lips start on both sides of the fracture surface. The shear lips grow in width on further crack growth until (almost) the total crack surface has become slanted. The start and growing in width of the shear lips is accompanied by a decrease in crack growth rate, resulting in a change to a lower slope of da/dN-ΔK on double-logarithmic scale. When the shear lips cover the total fracture surface the slope of da/dN versus ΔK changes again to a higher value. It is investigated if the development of shear lips is the cause of the decrease in crack growth rate. The answer to that question is different for both materials. Also some other transitions in the crack growth rate, i.e. slope changes in log(da/dN)-log(ΔK) will be studied in this paper. A possible explanation is given for a number of transitions. A simple model is made in order to predict fatigue crack growth behaviour in the shear lip area. The model is also applied to a situation with underloads in AA 2024-T351.

KEYWORDS

crack closure, shear lips, corrosion, environment, underloads, crack growth prediction

INTRODUCTION

Fatigue crack growth properties of two aluminium alloys, AA 2024 and AA 5083, are studied. The AlCuMg Aluminium Alloy AA 2024 is widely used in both civil and military aircraft because of its superior damage tolerance and fatigue properties. The AlMgMn Aluminium Alloy AA 5083 is increasingly used in shipbuilding, including high-speed ferries, because of its good mechanical properties and excellent corrosion (fatigue) resistance. Both materials have been fatigued in laboratory air. Besides that AA 2024 is also tested in vacuum and AA 5083 also in seawater. Crack closure was accounted for by varying the stress ratio. Especially transitions in the crack growth rate, that are accompanied by developing shear lips, form a subject of study. The transitions are an indication for a change in crack growth mechanism. For reliable fatigue crack growth prediction models it is important not only to have constant amplitude calibration data, but also to know the physical (micro) mechanisms involved. When ΔK at the beginning of constant amplitude crack growth is not too large, the crack grows with flat crack surfaces. At higher ΔK the crack becomes slanted, because shear lips start to grow from the surface inwards. The shear lips grow in width as the crack length increases. However there exists no direct correlation between a lower increase in crack growth rate and the

growing shear lip width, because it is shown that suppression of shear lip initiation and growth also shows the same transitional behaviour in the crack growth rate. For both materials the shear lip starts at about the same crack growth rate da/dN, at which value also the slope change to a lower value in log(da/dN)-log(ΔK) occurs, but both events are dependent on the environment. When the shear lips cover the total fracture surface the slope of da/dN versus ΔK changes again to a higher value.
A simple model is made in order to predict fatigue crack growth behaviour in the shear lip crack growing area. The principle of the calculation is that the crack growth rate da/dN and the shear lip width are both influenced by an unknown (micro) mechanism. The large change in slope of the log(da/dN)- log(ΔK) relation at the T3 transition point[1] is contributed to a change in environmental influence on the crack growth resistance or crack growth driving force. The increasing shear lip width is considered to be a measure for this change in environmental influence.
It will be assumed that the developing shear lip width rate is proportional to the difference in actual shear lip width and the equilibrium shear lip width, the latter being the width as would be found in a constant ΔK test after a large enough crack growth.
Furthermore the model is applied to a situation with underloads in AA 2024. The underloads are high enough to give rise to slanted crack growth. The crack growth behaviour after a large numbers of underloads is both measured and predicted. Differences in shear lip behaviour of both Al Alloys are discussed.

EXPERIMENTAL DETAILS

The yield stress (MPa) and chemical composition of the materials is as shown in the table:

TABLE yield stress and chemical composition (wt%) of the materials, remainder Al

AA	σ_{ys}	Mg	Mn	Si	Fe	Cr	Cu	Zn	Ti
5083	240	4.5	0.65	0.26	0.22	0.09	0.09	0.06	0.03
2024	395	1.40	0.70	0.06	0.20	0.01	4.43	0.06	0.02

The center-cracked specimens have a length of 340 mm, a width of 100 mm and a thickness of 8 mm (AA 5083) or 5 or 6 mm (AA 2024). Some of the AA 5083 test specimens have scratches on the side surfaces, parallel to the crack growth direction. The fatigue crack growth experiments are performed on a computer-controlled servohydraulic fatigue machine. The loading program is offered to the machine in the form of a table where the maximum load, the minimum load, the crack length and the frequency are specified. Thus the table specifies at which crack length load and frequency wil get new values. The table can be divided into small steps of crack length when needed. The crack length is measured using a pulsed direct-current potential drop measurement system. The frequency is 10 Hz, unless specified otherwise.

RESULTS

The results from 11 constant load amplitude tests on material AA 5083 in air are shown in figure 1. It can be noticed that at about da/dN = 0.1 μm/cycle, the crack growth rate curves gradually change in slope. Observations of the different fracture surfaces revealed that at the corresponding ΔK-values the crack appearance started changing from flat to slant.

[1] T3 is defined in figure 5

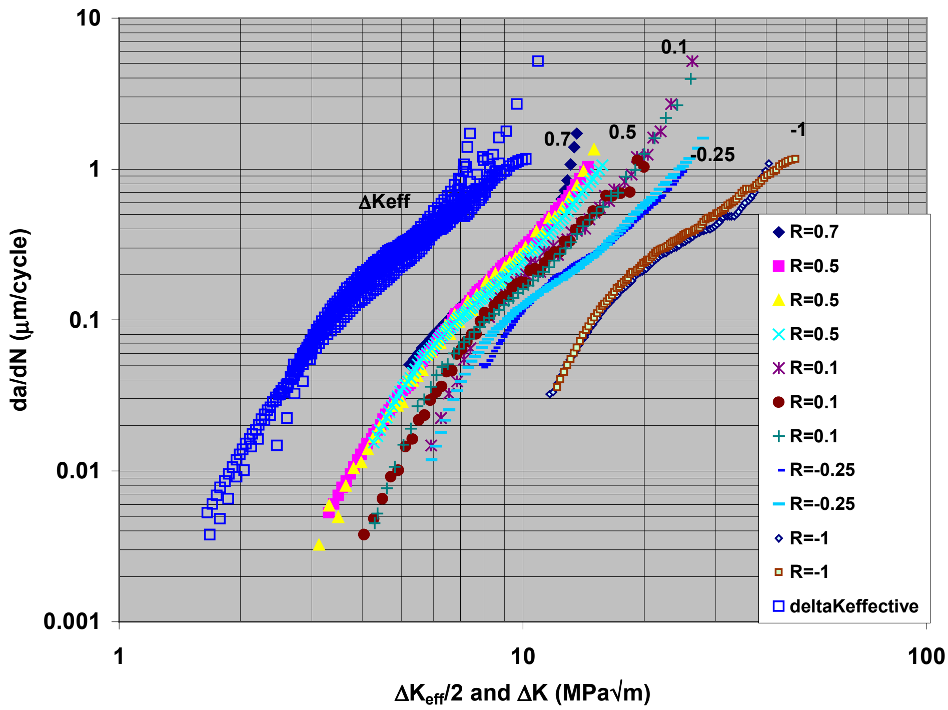

Figure 1. Results of 11 constant amplitude tests on AA 5083 at 5 different values of R and the corresponding da/dN-ΔK_{eff} (shifted a factor 2 to the left for clearness).

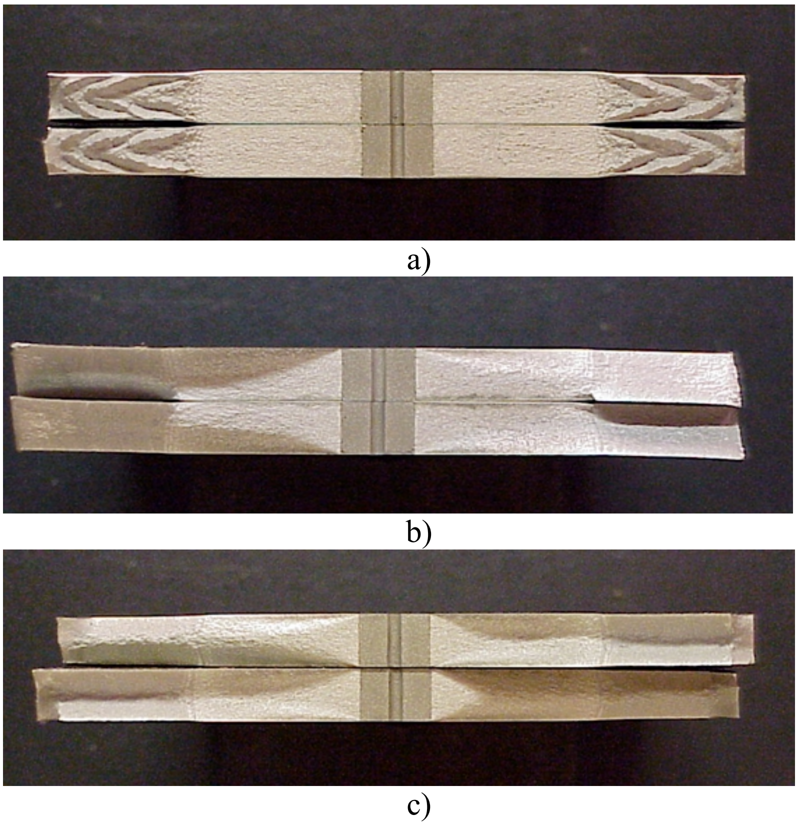

Figure 2. Shear lips on fatigue fracture surfaces in AA 5083, a) suppressed on both sides , b) on one side and c) not suppressed . P_{max}=95 kN, R=0.1, f=1 Hz.

In figure 2 fatigue fracture surfaces in AA 5083 are shown. A very high load of P_{max} =95kN , i.e. S_{max}=119 MPa, is applied. The frequency is taken as 1 Hz, in order to get enough datapoints. Although there is a tendency to form large shear lips, they can be suppressed by making scratches of 0.1 mm deep along the crack growth direction. In figure 2a this is done on both sides of the specimen, and in figure 2b only on one side. No scratches were applied on the specimen shown in figure 2c

In figure 3 the resulting da/dN-ΔK relations of the three tests of figure 2 are shown. The three tests shown in the figures 2 and 3 are a result of crack growth in a very high ΔK loading regime, where shear lips will start immediately if not suppressed. Hardly any difference is found in crack growth rates between specimens with scratches on both sides, where shear lips were fully suppressed, or specimens with shear lips on one side or specimens with full shear lips.

SHEAR LIP BEHAVIOUR OF AA 2024 AND AA 5083

It was shown in reference [1] that in a constant ΔK test shear lips grow in width until an equilibrium width has been reached. A linear relation was found between equilibrium width and the applied constant ΔK_{eff} for AA 2024:

$$t_{s,eq} = 0.67\Delta K_{eff} - 3.72 \text{ (mm)} \qquad (1)$$

For AA 2024 the well-known relation of Elber will be used for ΔK_{eff}=UΔK, with U=0.5+0.4R for – 0.1 < R < 0.7.

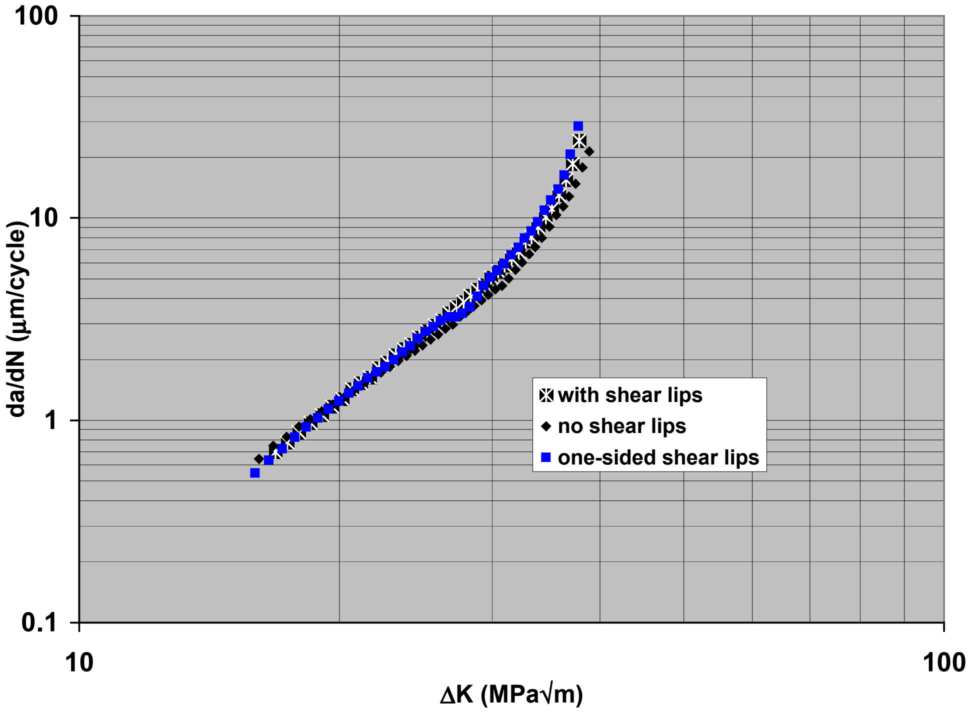

Figure 3. The corresponding da/dN-ΔK results for the three cases of figure 2.

If the actual shear lip width t_s and ΔK_{eff} do not fulfill this equilibrium equation, the shear lip width will increase or decrease until the equilibrium situation, i.e. $t_s = t_{s,eq}$, is reached. The rate of change in shear lip width is taken proportional with the difference in actual width and equilibrium width, in formula form:

$$dt_s/da = C(t_{s,eq}-t_s) \qquad (2)$$

It means that the shear lip width will change faster when the difference of equilibrium width and actual shear lip width is higher. For C the following equation was found for AA 2024 ($t_{s,eq}$ >0):

$$C= 0.22/t_{s,eq} + 0.08 \quad (mm^{-1}) \tag{3}$$

A similar behaviour for AA 5083 was assumed. Based on a preliminarily study of the fracture surfaces the equilibrium shear lip width is estimated:

$$t_{s,eq} = 0.90\Delta K_{eff}–5 \quad (mm) \tag{4}$$

For AA 5083 the C-value is estimated as:

$$C= 0.40/t_{s,eq} \quad (mm^{-1}) \tag{5}$$

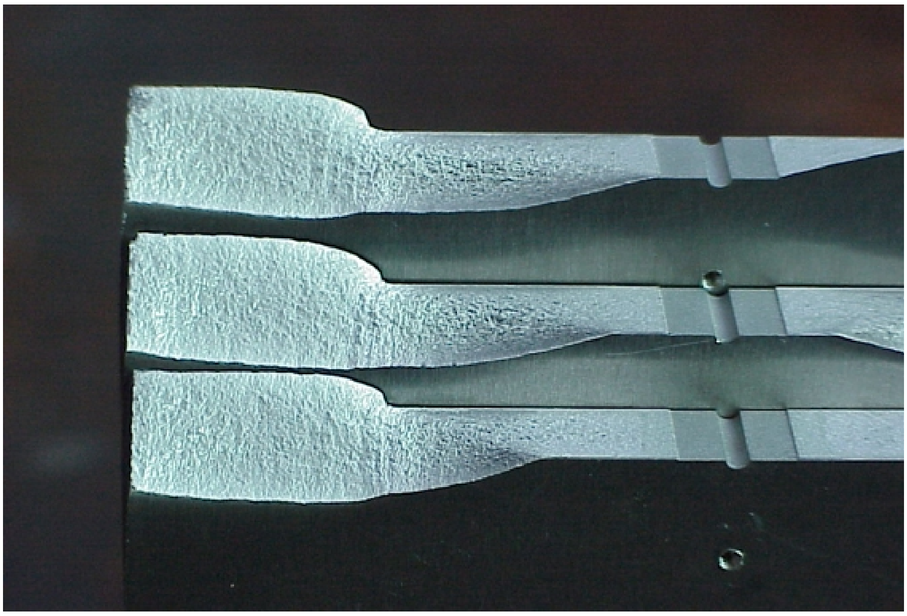

Figure 4. Shear lip suppressed completely on one side and partially on the other side, material AA 5083, S_{max}=119 MPa, R=0.1, f=1 Hz. Start shear lip at about a= 5, 10 or 15 mm crack length respectively.

In a constant amplitude test the ΔK_{eff} changes, i.e. increases, continuously and hence also the equilibrium shear lip width $t_{s,eq}$ and the actual width t_s. It means that t_s lags behind $t_{s,eq}$ for the growing crack. Only in a constant ΔK test the equilibrium shear lip width can be found.
In figure 4 three fracture surfaces are shown with partly suppressed shear lips on one side. Notice that the shear lip width increase is much faster when the shear lip is longer suppressed by the scratch. This is in accordance with equations 1 and 2, because $t_{s,eq}$ is higher at larger crack lengths for constant amplitude loading, while t_s is initially zero due to the shear lip suppressing surface scratches.

CRACK CLOSURE RELATIONS

For AA 2024 the crack closure relation of Elber is used. This relation fits the results for AA 5083 not very well. Crack closure for this alloy is not measured directly, but it is found by correlating 7 of the 11 constant amplitude da/dN versus ΔK results shown in figure 1. One test at R=0.7, one test at R=0.5, two tests at R=0.1, one test at R=-0.25 and two tests at R=-1. The best quadratic crack closure function $U= a+bR+cR^2$ is found by taking all combinations of a, b and c, within certain boundaries, and calculating $\Delta K_{eff}=U\Delta K$ for all measurement points of the 7 tests. For each combination of a, b and c a power formula of type $da/dN=C\ \Delta K_{eff}^m$ is fitted through the da/dN-ΔK_{eff} points. The combination of a, b and c with a maximum value of the correlation coefficient, based on log(da/dN) and log(ΔK_{eff}), is considered the best combination. However this method does not result in one solution, because all U'=constant*U do have the same correlating abilities. A single solution of U can be found by adding a constraint to the problem. The results in figure 1 show that the curves for R=0.5 and 0.7 are about the same, except at very high values of K_{max} where "static" fracture mechanisms are becoming important. It means that crack closure is not important, does not exist, above R=0.5. If it is assumed that U=1 already for R≥0.5, then this constraint can be added to the calculation procedure. The result of the calculation is $U=0.80+0.39R+0.03R^2$ for R<0.5 and U=1 for R≥0.5. With this constraint da/dN can be calculated as:

$$da/dN=0.41*10^{-3}\,\Delta K_{eff}^{2.8} \tag{6}$$

Note that this da/dN-ΔK_{eff} relation is the best fit through the da/dN-ΔK_{eff} points that show two slopes, one larger than 2.8 and one smaller, see figure 1. The same U formula can be used for both parts of the da/dN-ΔK_{eff} relation. This statement can easily be checked by applying the same crack closure calculation using only datapoints without shear lips, i.e. for da/dN<0.1 μm/cycle. For the constraint situation with U=1 for R ≥0.5, the result is now $U=0.80+0.39R+0.04\,R^2$ and

$$da/dN=0.40*10^{-4}\,\Delta K_{eff}^{4.17} \tag{7}$$

The U formula is almost the same, but the slope is of course higher. The da/dN-ΔK_{eff} fit result is shown in figure 1 for all data points at different R. A parallel shift by a factor 2 is applied to better show the result. Notice that by adopting that U=1 for R ≥0.5 means that also without a calculation the da/dN-ΔK_{eff} relation is known, because it is equal to all da/dN-ΔK relations for R ≥0.5. The result in figure 1 shows that this is indeed the case. The calculation was only needed for finding the U formula.

TRANSITIONS IN THE CRACK GROWTH RATE (AA 5083)

At first the change in slope at 0.1 μm/cycle was attributed to a possible different crack closure situation due to the growing shear lips. But it was shown in figures 2 and 3 that suppression of shear lips leads to hardly any difference in the da/dN-ΔK datapoints, thus extra closure due to shear lips probably doesn't exist in AA 5083. The start of the shear lips and/or change in slope is also probably not a matter of plane stress/plane strain, because the plane stress/plane strain situation depends on the plastic zone size, which depends on K_{max}.
The start of the shear lips and/or change in slope corresponds with different K_{max}-values (e.g. K_{max} = 23.3, 14.0, 8.9, 7.4 and 5.3 MPaŒm respectively for R = 0.7, 0.5, 0.1, -0.25 and -1). This means that the shear lips start at a large difference in plastic zone sizes for the different R-values, thus the size of the plastic zone can not be the cause of the slope change. In figure 5 other fatigue crack growth results for AA 5083 are shown. Three constant amplitude tests at R=0.1 are combined with a decreasing ΔK test, using ASTM E647, in order to show the da/dN-ΔK behaviour from the near threshold area at 10^{-4} μm/cycle until the very high value of 100 μm /cycle near instability. Five slope transitions, T1-T5, in log(da/dN)-log(ΔK) are shown. The slopes are 12, 3.2, 5.4, 2.5 and 3.6 for the numbered parts 1,2,3,4 and 5 in figure 5 respectively. The slopes are equal to the exponent of a power function that can be fitted through the corresponding da/dN-ΔK measurement points. In reference [2] much work has been done on fatigue crack growth of AA 2024. It is suggested in this work that the T3 transition occurs when the monotonic plastic zone size is about equal to the grain size. This is certainly not true for the fatigue crack growth in AA 5083 as we saw. Another proof that the transition T3 does not depend on the microstucture forms the fact that it occurs in several Al Alloys at the same da/dN in air. The only obvious correlation of T3 is with the crack growth

rate or, which is equivalent, with the ΔK_{eff}. The slope transition T3 starts at ΔK_{eff} =6.4 MPa $\sqrt{m}$, see figure 1. Note that this value corresponds well with the ΔK value for R=0.7 at da/dN=0.1 μm /cycle.

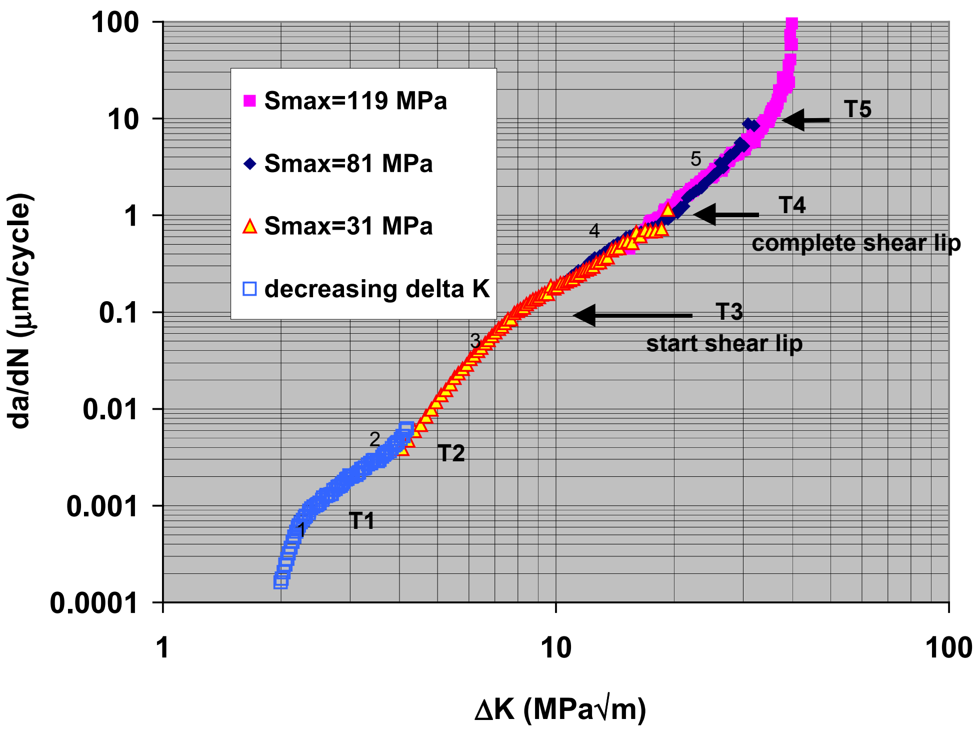

Figure 5. Experimental fatigue crack growth rate results for AA 5083 at R=0.1

In this paper we will concentrate on the slope transitions T3, T4 and T5. At T3 the slope decreases from 5.4 to 2.5, at T4 the slope increases from 2.5 to 3.6. Above T5, at about 10 μm/cycle, da/dN increases very fast towards instability. At the transition T3 shear lips start to grow, from the surface inwards. At T4 the fracture surface has become totally slanted, however it may be that the shear lip angle is still growing after T4. The shear lip angle has to be measured yet.

CRACK GROWTH PREDICTION MODEL

As was shown, the shear lip can not be the cause of the change in slope T3 of the log(da/dN)-log(ΔK) line. Therefore, there will be another, not yet known mechanism, that results in both shear lip start and growth and also in a lower slope of the log(da/dN)-log(ΔK) relation. But both events, shear lip start and slope change have no direct mutually dependency. They both depend on the unknown mechanism. In order to allow for quantitative crack growth rate calculations, the shear lip width is assumed to represent, to be a measure for, this unknown mechanism. Or even better, we assume that the transverse crack front length, which has a relation with the shear lip width, will be a measure for this unknown mechanism.
Thus da/dN, or equivalently the crack driving force ΔK, is influenced by the slope changing mechanism, for which the transverse crack front length is a measure. In the shear lip area the transverse length l increases when shear lips become wider or more slanted:

$$l = t + 2(\sec\vartheta - 1)t_s \quad (8)$$

where Ý is the shear lip angle, the angle with the original flat fracture surface and t the specimen thickness. ΔK is assumed to be inversely proportional to this length, i.e. the product of ΔK and the transverse crack front length l is assumed to be constant:

$$\Delta K\, l = \text{constant} \tag{9}$$

A larger shear lip width means a higher l , and thus a lower ΔK and a lower da/dN. The calculation will be applied for a constant amplitude test. For this test the tranverse crack length will increase as the crack grows. For the calculation of the applied ΔK the ASTM formula for a centre-cracked tension specimen (width w) is used:

$$K = \sigma\sqrt{\pi a}\sqrt{\sec\frac{\pi a}{w}} \tag{10}$$

At higher da/dN "static" effects are probably superposed on the fatigue crack growth rate. The "static" effects can be added to the calculation by correcting the ΔK for the increased plastic zone at the tip. In metals the fatigue crack growth is accompanied by plastically deformed material on the crack flanks due to the high stress concentration at the fatigue crack tip. The plane stress monotonic plastic zone size at the fatigue crack tip can be given as:

$$2r_p = \frac{1}{\pi}\left(\frac{K_{max}}{\sigma_{ys}}\right)^2 \tag{11}$$

σ_{ys} is the yield stress of the metal and r_p is the radius of the (assumed circularly) plastic zone. The plastic zone size is dependent on the stress situation at the crack tip, for a plane strain situation the plastic zone size is assumed to be about a factor 3 smaller that the plane stress zone. For the moment we neglect this phenomenon, because the crack growth resistance and the shear lip development are more dependent on the specimen surface, where plane stress prevails.

It can be proved that the crack behaves as if it were r_p longer due to the plasticity. The new crack length corrected for plasticity thus becomes $a + r_p$ instead of a. According to eq.(10) this will give a higher K (and thus a higher K_{max}). On its turn this higher K_{max} will give a higher r_p, etc. When the crack length and the plastic zone size are not too large this iteration of r_p and K_{max} will converge to stable end values. r_p is solved from:

$$2r_p - \frac{K^2_{max,applied}(a+r_p)}{\pi a \sigma^2_{ys}}\frac{\cos(\frac{\pi a}{w})}{\cos(\frac{\pi(a+r_p)}{w})} = 0 \tag{12}$$

$K_{max,applied}$ is defined as the maximum value of the applied K, using eq. 10, without plasticity correction. The calculation of r_p is numerically performed using regula falsi for every a. ΔK is calculated, using the r_p value from eq.(12) as:

$$\Delta K = (1-R)K_{max,applied}\sqrt{1+\frac{r_p}{a}}\sqrt{\frac{\cos(\frac{\pi a}{w})}{\cos(\frac{\pi(a+r_p)}{w})}} \tag{13}$$

The ΔK calculation involves both the shear lip correction, eqs 1-4 and 8, as well as the "static" correction, eq 12. Hereafter da/dN is calculated, using the da/dN-ΔK_{eff} equation in the crack growth area without shear lips, eq.7.

RESULT OF THE CRACK GROWTH RATE PREDICTION

The prediction is tested on crack growth rate results for R=0.1 and R=0.5, as shown in figure 6. In this figure the results of three constant amplitude tests at R=0.5 and four constant amplitude tests at R=0.1 are compared with the calculated da/dN-ΔK prediction relation.

A POSSIBLE EXPLANATION OF THE CHANGES IN SLOPE AT T3, T4 AND T5

The following explanation is rather speculative at the moment, but it can explain most of the results. It is found in figure 1 that in AA 5083 the change in slope at T3 starts at 0.1 μm/cycle in air at 10 Hz. It is also found that it occurs at 0.2 μm/cycle in seawater, also at 10 Hz [2]. The same is true for fatigue crack growth in AA 2024 in air and seawater [3]. Fatigue crack growth tests in AA 2024 in vacuum have no change in slope. This is shown in figure 7. In figure 7 two constant amplitude tests on 5 mm thick AA 2024 T351 are shown, performed at 20 Hz in vacuum. No changes in slope are visible. The crack appearance is slanted and rough from the beginning of crack growth.
The change in slope at T3 is found to be independent of K_{max} or ΔK, but it is dependent on da/dN, which is equivalent to dependency on ΔK_{eff}. These results indicate that the reason of the change in slope at T3 is not due to mechanically causes alone, but that it also depends on the environment.
Suppose that some corrosion reaction is responsible for enhanced fatigue crack growth rate below the transition T3, i.e. below 0.1 μm/cycle in air. And suppose that above this crack growth rate the crack moves too fast for the corrosion assisted mechanism to take fully place. Then the intrinsic (true) fatigue crack growth rate will increasingly dominate at higher crack growth rates, with a growing slanted crack surface as a result. Seawater is a more aggressive environment than air, and it can be expected that a higher crack growth rate than in air is needed to outrun the corrosion reaction speed. Therefore T3 lies at a higher da/dN in seawater. In vacuum the reverse is true and a lower da/dN at T3 can be expected. However it may be that there is no transition T3 at all in vacuum (probably in practice the vacuum is not good enough and it will take place at a very low value of the crack growth rate). We will at the moment not speculate on the exact mechanism of the corrosion reaction, but following this rationale it is clear that the fatigue fracture situation with shear lips is the true (i.e. without corrosion assistance) fatigue crack growth mode in these Al Alloys. When the fracture surface is flat, it is so by an environmental attack.

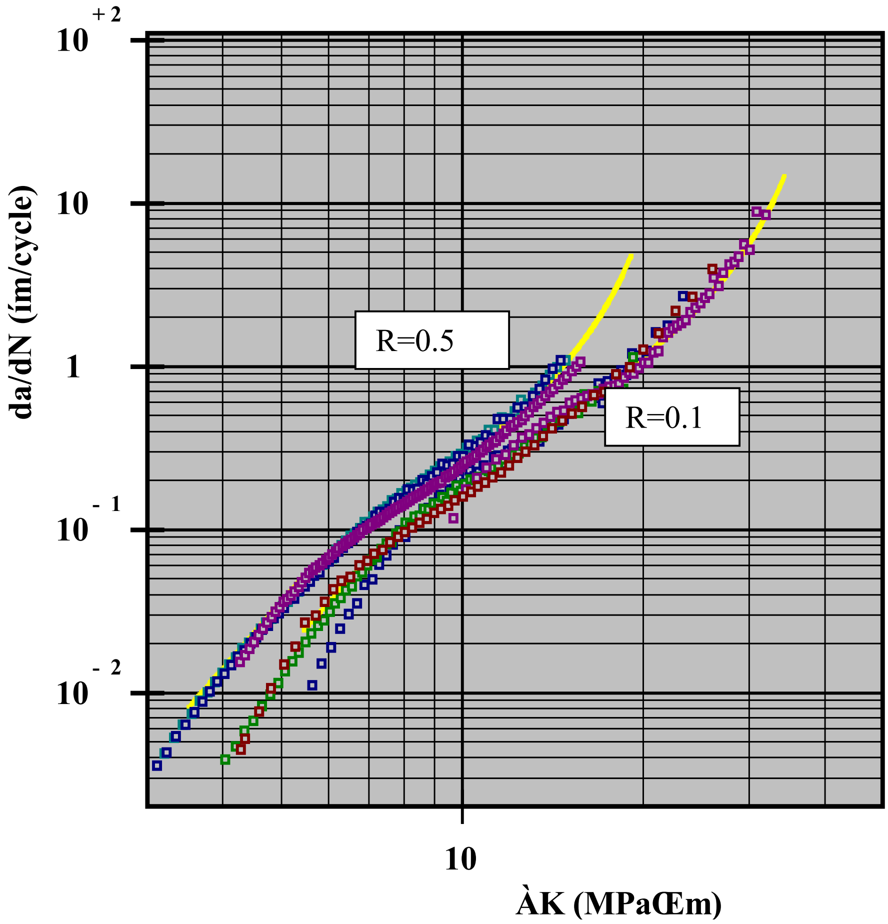

Figure 6. Prediction lines and measurement points at 10 Hz for R=0.1 and R=0.5, material AA 5083.

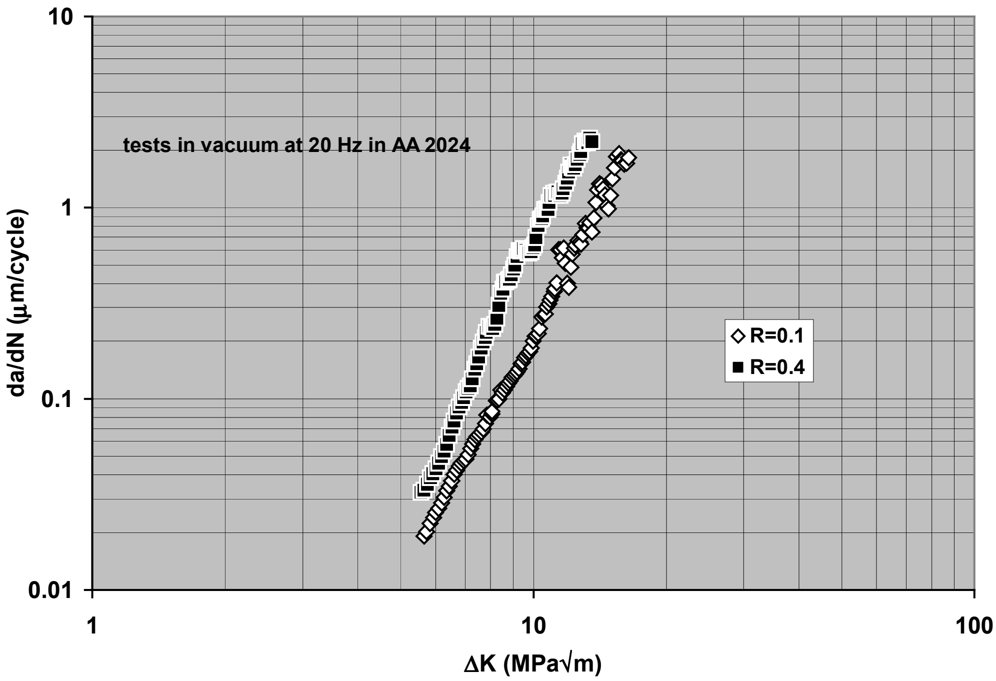

Figure 7. Results of 2 constant amplitude tests on AA 2024 in vacuum (10^{-5} Torr) at 2 values of R.

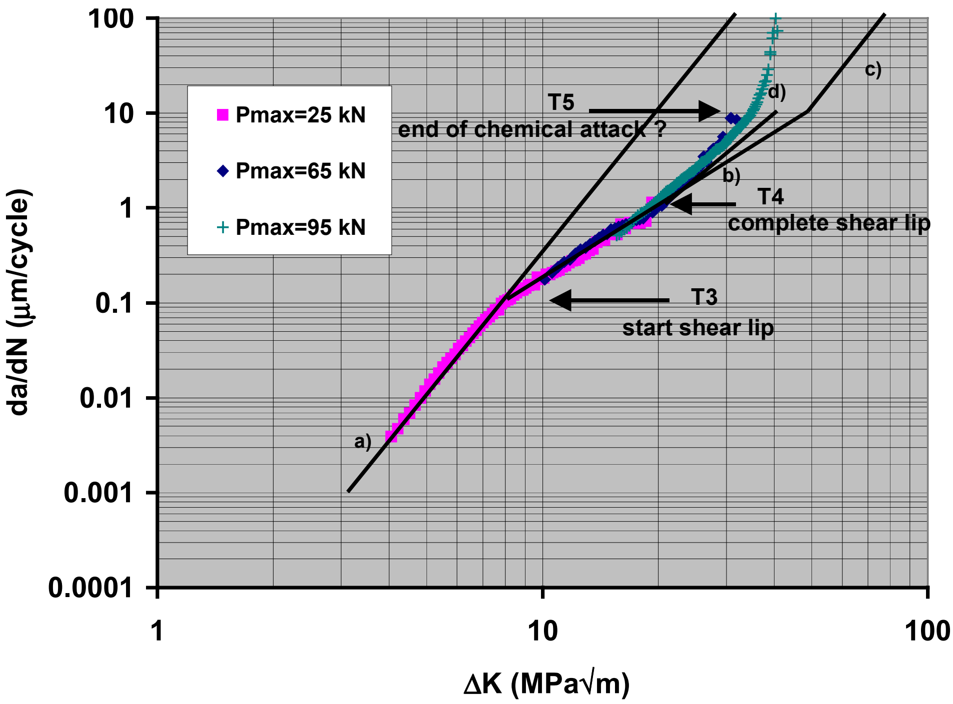

Figure 8. Possible explanation of the slope transitions T3, T4 and T5 in the log(da/dN)-log(ΔK) relation due to a change in chemical attack, at T3 the chemical attack is maximal, at T5 the chemical attack has become zero.

The principle of the rationale is shown in figure 8, which figure has some data from figure 5. It is assumed that when the environment is agressive enough, the log(da/dN)-log(ΔK) relation will be linear, line a) in the figure, except at very high ΔK when "static" effects can be expected. At the transition point T3, where shear lips start, the crack growth rate begins to outrun the corrosion (chemical) attack. A decrease in da/dN, compared with line a), gradually develops when ΔK increases, line b), until a maximum decrease is reached. This maximum decrease in da/dN is reached when the true fatigue crack growth rate completely outruns the chemical attack. When no "static" corrections have to be applied, we would have followed line b), until the sharp transition where b) is followed by c). At this sharp transition of line b) to line c) the chemical attack is ended and the crack growth rate resumes its original slope. This transition marks the different inluence on da/dN of a decreasing chemical attack along line b) and the absence of chemical attack along line c). A drawback is that in reality there are slope changes at T4 and T5. The slope of the da/dN measurement points is lower than that of line a) between T4 and T5, and higher after T5. Although the observation is difficult, it seems that near the transition T4 the shear lips cover the whole fracture surface. At the moment it is not clear if this coincidence of maximum shear lips and transition T4 is accidentally or that it has a physical reason. It is also not clear at this moment if the shear lip angle is constant or that it increases after T4.

There are two possible explanations why there are slope transitions at T4 and T5. The first has to do with the shear lips. At T4 the fracture surface is completely slanted, but the shear lip angle is probably less than 45°. The transverse crack length can still increase after T4 due to further increase of the shear lip angle, but the rate of transverse crack length increase has become lower than before T4. Thus ΔK (and da/dN) can still decrease due to this effect after T4, but the rate of decrease is lower than before T4, leading to a somewhat higher slope after T4. This is shown in figure 8 by the line indicated with d).When the chemical attack has ended in principle the original slope of line a) will be restored. On all parts however there is also an increase of da/dN due to "static" corrections, which is becoming increasingly more

important at higher ΔK. Therefore we get a sharp transition at T5, which is build up of the sharp transition of line b) to line c), plus the "static" corrections of da/dN. The slope just before T5 is lower than the original slope of line a).After T5 the slope is higher than that of line a).
The second explanation is based only on "static" corrections of da/dN applied on lines b) and c). The correction becomes larger for higher ΔK. Transition T4 is then only a fake transition and marks a situation where the "static" correction is becoming more important. At T5 the explanation stays the same. Here the environmental effect has ended, and both effects, i.e. end of chemical attack and "static effect", are superposed leading to very fast crack growth and instability.
Resuming we can say that the lower slope between transition points T3 and T4 in figure 8 is due to a gradually change from full (100%) corrosion assisted crack growth at T3 to very low chemical attack above the transition point at T4. The change in chemical attack between T3 and T4 (T5) causes a change in da/dN decrease in this area of crack growth leading to the lower slope in log(da/dN)-log(ΔK).

EFFECT OF THE FREQUENCY ON THE TRANSITIONS.

There is a problem in the reasoning given above. It was found that frequency had hardly any effect on fatigue crack growth rate in AA 5083 in air. The same da/dN-ΔK curves were found for frequencies of 10 Hz, 1 Hz and 0.1 Hz. However the T3 slope transition was in all cases at about 0.1 μm/cycle. That means that the slope transition occurs at very different crack growth rates per time unit, i.e. da/dt=f*da/dN, while it is generally assumed that corrosion fatigue is a time-dependent phenomenon. A solution to this dilemma can be found in the cyclic nature of the fatigue process. When a frequency of 10 Hz is applied, we have 10 pieces of discontinuous crack growth per second, because crack extension in metals only occurs during the increasing part of the loading cycle. At the maximum load a lot of blunting is present. The blunting prevents most of crack growth during the decrease of the load. The load decrease however sharpens the crack by compression (crack closure). Therefore the next load increase will meet with a sharpened crack and a corresponding high stress concentration, resulting in a new crack advance. This process of discontinuous crack growth is repeated in every cycle (in the "linear" log(da/dN)-log(ΔK) area of crack growth). The corrosion-assisted mechanism will only work during the crack extension period of the loading cycle. During load decreasing the crack tip will be shielded by crack closure, which effect will remove active corrosion species out of the crack tip area. In the next cycle the active species has to move to the fresh crack tip again. For a corrosion effect to take fully place the active corrosion species has to move faster then the crack opening and the following crack extension per cycle, i.e. da/dN. Thus when da/dN starts to outrun the corrosion reaction speed the slope transition can start. And a high da/dt, made up of a high frequency and a low da/dN, will not change the slope. Even a da/dt difference by a factor of 100 will then not change the start of the transition. The start of the slope change in AA 5083 is thus only a matter of da/dN and not of da/dt. In AA 2024 the situation is somewhat more complicated as will be discussed next.

DIFFERENCES IN SHEAR LIP BEHAVIOUR BETWEEN AA 5083 AND AA 2024.

In figure 2 some fracture surfaces with shear lips in AA 5083 are shown. The shear lips have a smooth appearance. Tests at different frequencies did not change the smoothness of the shear lips. Only the "static" overload fracture in figure 2a shows rough shear lips. The shear lips in AA 2024 sometimes are smooth and sometimes they are rough, comparable with the "static fracture surface in figure 2a. They are rough for frequencies above about 2.5 Hz, while below 1 Hz they are smooth, see figure 9. It was shown [6] that the rough fracture surfaces experienced more crack closure and a lower da/dN. Due to this effect the fatigue crack growth in AA 2024 is frequency dependent, unlike in AA 5083. Compared with AA 5083 this material has two da/dN retarding mechanisms above the T3 transition point, the first due to the decreasing environmental influence and the second due to extra crack closure of rough shear lips at higher frequencies. Unfortunately at this moment not enough constant amplitude data around T3 are available for AA 2024.

UNDERLOADS IN AA 2024

Constant ΔK tests with constant ΔK underloads were performed in AA 2024. The underloads were high enough to lead to development of shear lips, while the ΔK before and after the underloads were to low for it. All K_{max} were the same to avoid a change in plasticity induced crack closure at the loading transitions. The principle is shown in figure 10.

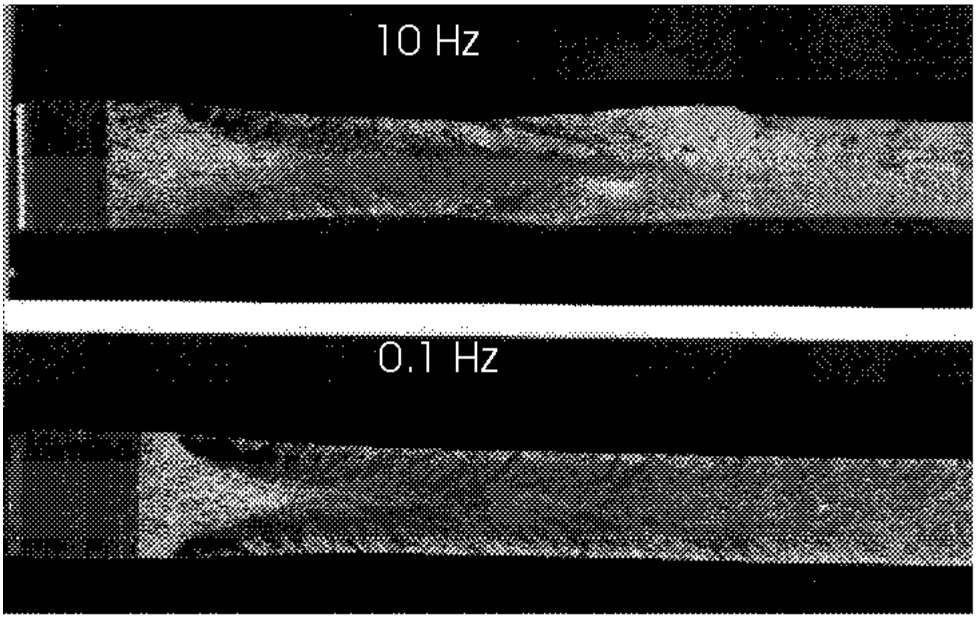

Figure 9 Examples of rough and smooth shear lip crack surfaces at test frequencies of 10 Hz and 0.1 Hz.

Both constant ΔK values have been carefully chosen to yield a fracture surface with shear lips in the case of underloading, and no shear lips before and after the underloads. The low constant ΔK_{eff} value is 5 MPa√m. For the high ΔK_{eff} of the underload cycles ΔK_{eff} = 16 MPa√m is used. Here it is also found that when shear lips develop in AA 2024 there is an effect of the frequency of the underloads on da/dN and on the retardation afterwards. This is shown in figure 11. Rough shear lips are assumed to have an effect on the ΔK_{eff} . The length of the tranverse crack front is assumed here to be also a measure for the effect of rough shear lips on crack closure. For the calculation again $\Delta K. \ell$ = constant is assumed, with ℓ the length of a transverse section of the crack front. It is possible to predict the a-N behaviour after the underload tests by integration of a da/dN-ΔK_{eff} relation, found from constant amplitude tests. Retardation in crack growth rate was measured after the underloads. The retardation was larger for higher ΔK of the underloads and for more underload cycles, see figure 12. The shear lips vanished quickly after the underloads, but the retardation of the crack growth rate lasted about three times as long, i.e. if there is an effect of the shear lips on ΔK, it extends outside the area where shear lips are really present.

The same calculation is applied as on AA 5083. Only now, in this situation of decreasing and vanishing shear lip width, ΔK is not assumed to be influenced only by the real shear lip width at the crack tip, but by a mean of the shear lip width extending over some mm crack length after the tip. Thus some history dependence is build into the calculation procedure, for this history of decreasing shear lip width. Calculations taking the actual shear lip width at the tip as a measure for ΔK, and calculations taking the mean shear lip width over 3 mm after the tip were applied and compared with a real test with underloads. The 3 mm was estimated using a potential drop measurement of the affected crack length by early contact, due to crack closure, see figure 13. Just after the load transition the affected length of 3 mm can be measured. The effect decreases fast due to oxidation of the surfaces. The measured and predicted a-N is shown in figure 14.

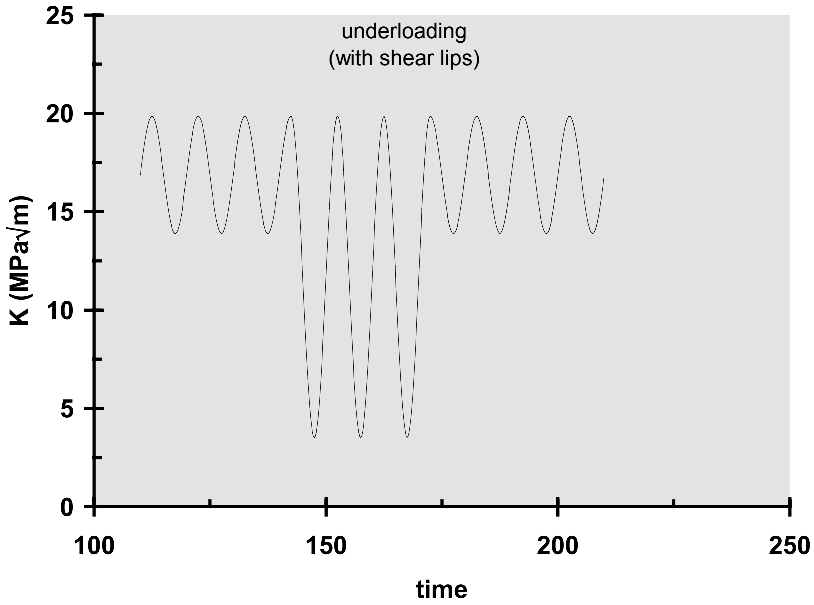

Figure 10. Principle of underload tests

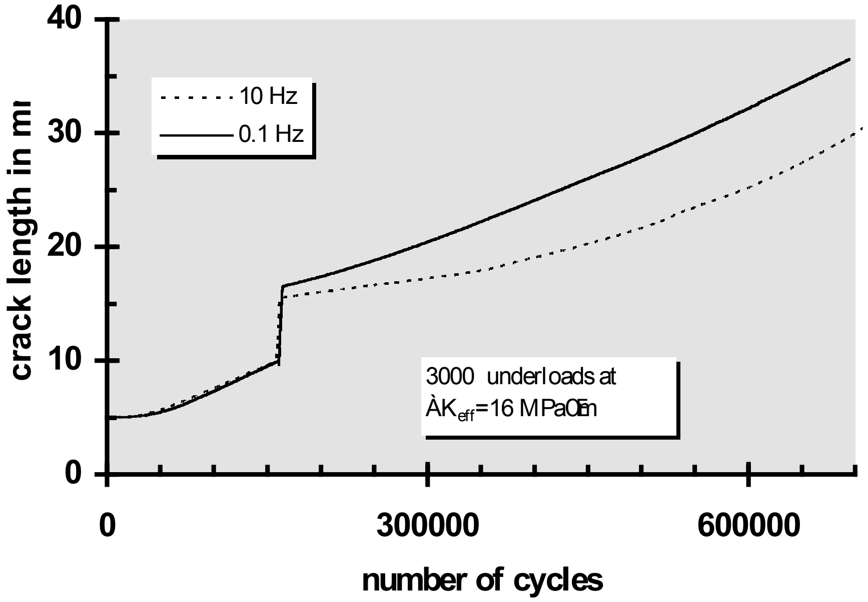

Figure 11. Frequency effect shown in tests with 3000 underloads in AA 2024,

CONCLUSIONS

1) The development of shear lips is not necessarily the cause of the slope change in the log(da/dN)-log(ΔK) at transition T3.
2) Slope change and development of shear lips are both the result of a decreasing chemical attack above transition point T3.
3) The T3 and T4 transitions are environmentally dependent
4) The T3 transition is only dependent on da/dN and not on da/dt.
5) The crack growth rate predictions are reliable, thus the shear lip width is a good measure for the transition from fast, environmentally assisted, crack growth rate to slower intrinsic true fatigue crack growth rate above the transition point T3.
6) The enhanced crack growth rate at lower da/dN, i.e. below T3, is due to environmental attack.

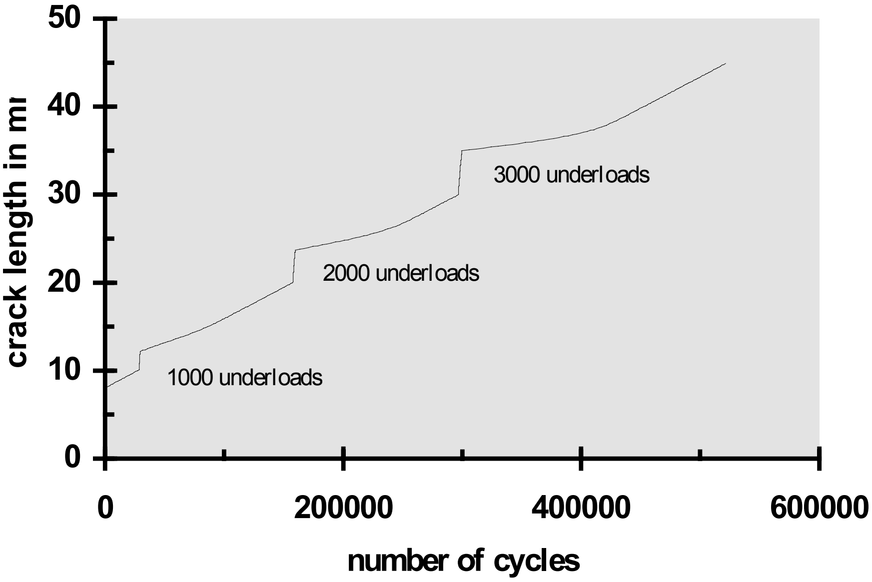

Figure 12. Calculation of a versus N at different numbers of underloads

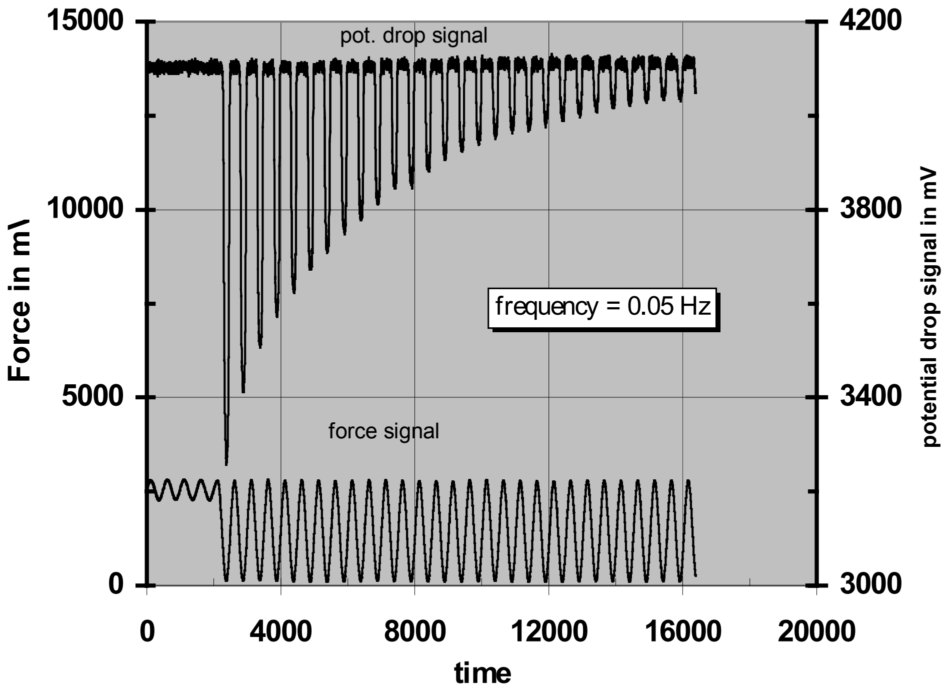

Figure 13. Measurement of affected crack length at the underloads.

ACKNOWLEDGEMENTS

The authors express their gratitude to the students Yves Franchimon and Jeroen Scheepmaker, and to the former student Adi Hascaryantono. We also thank professor Jaap Schijve and ir Saskia de Vries for careful reading and comment.

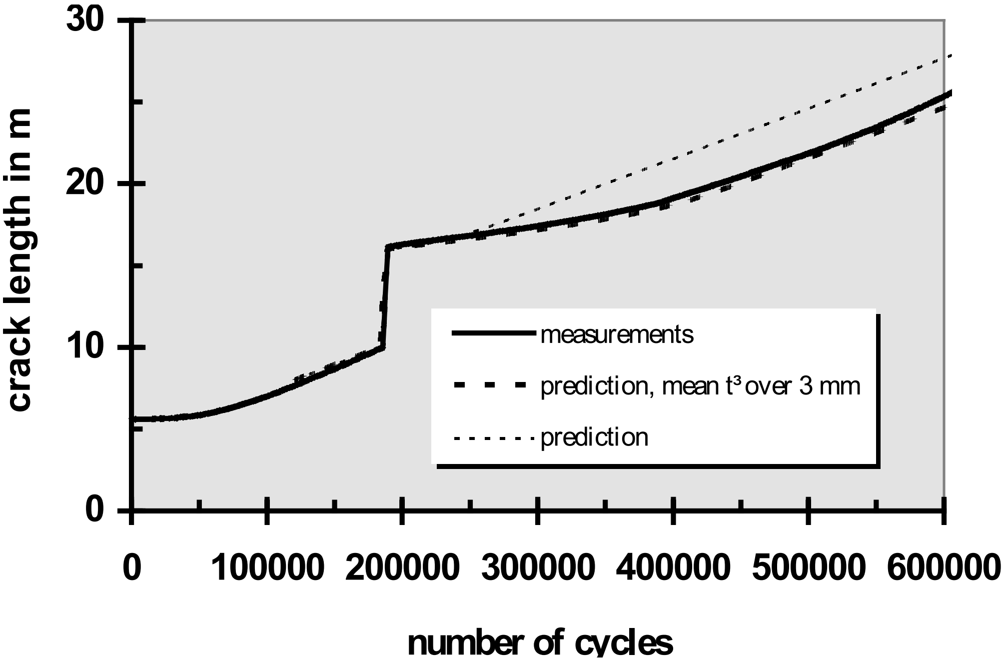

Figure 14. Measurements and prediction of the a-N curve in AA 2024 with 5000 underloads, underload sequence ΔK=5-16-5 (MPa√m) at K_{max} = 29 (MPa√m) and 10 Hz.

REFERENCES

[1] Zuidema, J. and M. Mannesse, *A model for predicting slant crack growth in Al 2024*. Engineering Fracture Mechanics 34 ,1989, 2, p.445-456'

[2] Wanhill, R.J.H, *Damage Tolerance Engineering Property Evaluations of Aerospace Aluminium Alloys with Emphasis on Fatigue Crack Growth*, report NLR TP 94177 L, 1995, Amsterdam, The Netherlands.

[3] Jan Zuidema, Saskia de Vries and Adirakhmantyo Hascaryantono,*The Accelerated ΔK Fatigue Crack Growth Test on AA 5083-H321 and Similitude Validation,*The 13th European Conference on Fracture ECF 13, 6th-9th september, 2000, San Sebastian, Spain.

[4] Zuidema, J., P.J.M. Mense and R.A.H. Edwards, *Environmental dependence of fatigue crack growth retardation following a single overload in 2024-Al alloy*. Engineering Fracture Mechanics 26 (1987) pp.349-356.

[5] Ton Riemslag, Kees van Kranenburg, Saskia Benedictus-de Vries, Fred Veer and Jan Zuidema, *Fatigue crack growth predictions in AA 5083 and AA 2024 using a simple geometric model*. Conf. Proceedings of 10TH International Congress of Fracture ICF10, Honolulu, USA, 3-7 december 2001.

[6] J.Zuidema and J.P. Krabbe, *The effect of regular and irregular shear lips on fatigue crack growth in AL 2024*, Fatigue Fract. Engng Mater. Struct. Vol. 20, No. 10, pp. 1413-1422,1997.